Vacuum Sorption Pumping Studies with Pure Gases on Molecular Sieves

Low-pressure, low-temperature adsorption of N_2 and CO_2 were studied in beds of 4A molecular sieves. System parameters were estimated by a comparison of experimental results and a molecular-flow theoretical model. Nitrogen data followed theoretical prediction. Theory adequately represented pressure above the bed for CO_2, while pressure drops deviated significantly from the model.

K. S. CRABB, J. J. PERONA,
C. H. BYERS, and J. S. WATSON

Chemical Technology Division
Oak Ridge National Laboratory
Oak Ridge, TN 37831
and University of Tennessee
Knoxville, TN 37996-2200

SCOPE

Cryosorption pumping of gases on deep beds of sorbents is becoming an important process in several areas of energy production, including storage of fuel gases and development of fusion energy. Sorption pumping differs from most sorption processes in that the goal is generally the uptake of all components, rather than separation. No carrier gas is used, and there is no forced convection through the sorbent bed. As sorption proceeds, the bed acts as a pump to transfer gas from a closed system.

Both current experiments and future applications of fusion energy require clean roughing pumps to evacuate chambers with volumes of up to 10^4 m^3 (Fisher and Watson, 1978). Large cryosorption pumps, in which gases are sorbed on deep beds of molecular sieves at liquid nitrogen temperature, are under consideration for this service; however, modeling of the heat and mass transport processes that occur as the gas is sorbed requires more detailed understanding. The purposes of this study were to obtain experimental results on deep-bed cryosorption and to compare these results with a theoretical model in order to provide estimates of transport and equilibrium properties of these systems. Experiments were carried out with nitrogen at 77 K and carbon dioxide at 198 K. Pressures ranged from 0.1 to 100 Pa (7.5×10^{-4} to 0.75 torr).

Numerous studies exist on the performance of fixed-bed adsorbers in which the controlling mechanism is diffusion into solid particles. Most investigations have considered isothermal sorption from dilute feed streams at standard conditions. The models predict effluent concentration as a function of time in response to a stepwise increase in sorbent concentration.

In the present study, pure gas drawn into the bed is in molecular flow. Velocity and pressure drop are related somewhat differently than in viscous flow, namely:

$$v = -\frac{\kappa}{p}\frac{\partial p}{\partial z}.$$

The parameter κ is a function of molecular speed and channel geometry, making it difficult to predict flow through the interstices of a packed bed.

Published data on gas diffusion in type 4A commercial pellets and, in some cases, on gas-solid equilibrium are available for much higher temperatures and pressures than those considered here. Extrapolation of such data to experimental conditions is subject to considerable error, and a need exists for experimental results obtained at the conditions of interest.

CONCLUSIONS AND SIGNIFICANCE

The general objective of the work was to develop a mathematical model to describe quantitatively the mass transfer in a deep-bed cryosorption pump. A set of equations describing these processes was derived from theory, and a numerical solution of the set was developed. Major assumptions in the theoretical model were: isothermal conditions, parabolic concentration profile within the sorbent particles, equilibrium adsorption isotherms represented in a Langmuir form, and concentration-independent solid diffusion controlled by either the intracrystalline or the macropore structure.

The model represents well the experimental data for nitrogen up to the point when the bed approaches saturation. Values of κ that best fit the experimental data are 8×10^{-3} m^2/s for a bed of 0.55 mm pellets and 1.05×10^{-2} m^2/s for a bed of 0.72 mm pellets; thus the value of κ is proportional to pellet size. The effective diffusivity for nitrogen in the solid phase is 5×10^{-12} m^2/s, which is very high compared to intracrystalline values extrapolated to 77 K. Apparently adsorption occurs only on the crystal exterior surfaces, and the effective diffusivity represents macropore diffusion.

For carbon dioxide, the model represents accurately the pressure-time curves above the bed but does not describe with great precision the pressure drop data across the bed. A value

Correspondence concerning this paper should be addressed to J. J. Perona.

for κ of 3.50×10^{-2} m²/s provides a good fit for the first 20 to 30 h of a run, but a value of about 2.00×10^{-2} m²/s yields better agreement over the total run time of about 120 h.

It is postulated that the controlling diffusion resistance for CO_2 is in the micropores of the pellets. The time constant (D/S^2) for diffusion of carbon dioxide was estimated to be 1.3×10^{-5} s^{-1}. Applying the mean crystal size of 1.85 μm, an effective diffusivity of 1.1×10^{-17} m²/s is obtained, which agrees well with extrapolated values from literature data.

THEORETICAL MODEL

Figure 1 sketches the physical system being modeled. A single-component gas flows at constant flux into a void space above a sorbent bed. The void space is at ambient temperature, while the bed is at the temperature of the surrounding bath. The system is initially under vacuum. In the work conducted here, the starting pressure was about 0.1 Pa.

As the gas molecules flow into the cooled bed, they are adsorbed on the porous sorbent particles. A pressure gradient is maintained across the bed, and gas continues to flow into the bed until the sorbent approaches saturation. Two transport processes occur as gas moves into the bed. Hydrodynamic transport takes place as gas flows through the bed interstices, and diffusive transfer occurs as adsorbed molecules move from the surface to the interior of the sorbent particles. The two transport processes can be related by a mass balance around a differential length of bed:

$$\epsilon \frac{\partial c}{\partial t} + \rho_B \frac{\partial \bar{q}}{\partial t} + \epsilon \frac{\partial (vc)}{\partial z} = 0. \tag{1}$$

For pure gases, the concentration, c, is equal to the molar density and, for ideal gases, is a linear function of pressure.

Because of the low temperatures and pressures and the small channel size, flow through the bed interstices is in the molecular flow regime. The relevant quantity used in describing the molecular flow of gases is the throughput, Q, which is the volume of gas at a known pressure and temperature passing a plane per unit time. This throughput is defined mathematically by

$$Q = pV_f = pvA, \tag{2}$$

For molecular flow through long tubes and channels, Knudsen (1909) derived the following expression for Q:

$$Q = -\frac{4}{3} \frac{v_m}{\int_0^L \frac{H}{A^2}\, dL} (p_2 - p_1). \tag{3}$$

The average molecular velocity, v_m, depends entirely on the temperature and molecular weight of the gas. The integral depends on the channel geometry. In using this equation to model flow through the interstices of a packed bed, where the channel is the void volume between particles, the integral is intractable. However, by estimating the ratio H/A^2 by an average value over the length of the channel, the average gas velocity can be represented by

$$v = -\left[\frac{4}{3} \frac{v_m}{\left(\frac{H}{A^2}\right)_{avg} A_{avg}}\right] \frac{1}{p_1} \frac{p_2 - p_1}{L}. \tag{4}$$

Values of the molecular speed, v_m, are 241 m/s for N_2 at 77 K and 309 m/s for CO_2 at 198 K. Because of the complex channel geometry, the group of constants represented by the symbol κ must be determined experimentally (Perona et al., 1983). For a differential length of channel, Eq. 4 becomes

$$v = -\frac{\kappa}{p} \frac{\partial p}{\partial z}. \tag{5}$$

Mass transport of a single-component gas within sorbent particles may be considered either a diffusional process or a hydrodynamic process (Ruthven and Loughlin, 1971a). We have chosen to model the solid-phase transport using an effective mass diffusivity (Garg and Ruthven, 1973). If the particles are represented as spheres, the governing equation is

$$\frac{\partial q}{\partial t} = \frac{D}{r^2} \frac{\partial}{\partial r}\left(r^2 \frac{\partial q}{\partial r}\right). \tag{6}$$

The assumption of spherical geometry is valid if macropore diffusion controls, but a cubic geometry would be more accurate if intracrystalline diffusion controls (Ruthven and Loughlin, 1971b). In the latter case, the accuracy of the results can be improved by taking into account the crystal size distribution. For this study spherical geometry was chosen and Eq. 6 was used.

The solid-phase concentration, q, varies with radial position within the particles. The quantity required in the material balance is the average loading per unit weight of sorbent, $\bar{q}$, at a given bed position and time; $\bar{q}$ is defined by

$$\bar{q} = \frac{3}{S^3} \int_0^S q r^2\, dr. \tag{7}$$

It is convenient to assume a parabolic form for the solid-phase concentration profile. This approximation has been used in adsorption and ion exchange work in the past and has generally given good results, e.g., Glueckauf (1955), Garg and Ruthven (1975), and Liaw et al. (1979). This assumption leads to a simple linear driving force expression

$$\frac{\partial \bar{q}}{\partial t} = \frac{15D}{S^2} (q_S - \bar{q}). \tag{8}$$

The use of Eq. 8 speeds up the numerical solution of the sorption equations substantially (Tung, 1977).

For a single-component system, no gas-phase resistance to mass transfer occurs at the particle surface, and q_S is the surface loading in equilibrium with the gas pressure. Garg and Ruthven

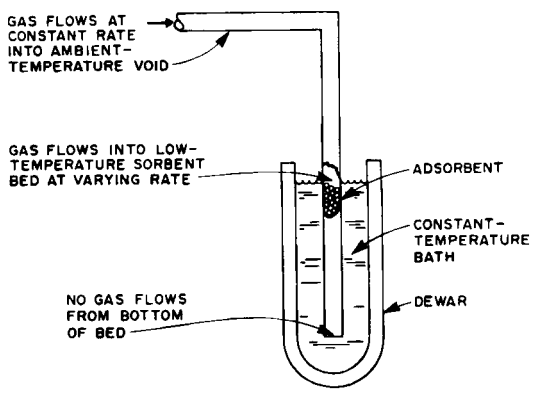

Figure 1. Gas flow in experimental sorption pumping system.

(1973) have shown that a Langmuir form of adsorption isotherm can successfully model surface adsorption in commercial synthetic zeolites. Thus,

$$\frac{q_s}{q_m} = \frac{kp}{1+kp}. \tag{9}$$

Garg and Ruthven also note that q_m and k should both be regarded as empirical constants.

The three dependent variables have now all been related to the one variable of the gas pressure in the bed. The expressions for c and v can be substituted into Eq. 1, yielding

$$\frac{\epsilon}{RT_b}\frac{\partial p}{\partial t} + \rho_B \frac{\partial \bar{q}}{\partial t} - \frac{\epsilon\kappa}{RT_b}\frac{\partial^2 p}{\partial z^2} = 0. \tag{10}$$

This equation, along with Eqs. 8 and 9, form the set that must be solved to model mass transfer in the bed in terms of pressure and solid loading.

Solution of these equations requires appropriate initial and boundary conditions. The initial conditions are

$$\text{At } t = 0, \text{ for all } z,\ p = 0 \text{ and } \bar{q} = 0. \tag{11}$$

The fluid-phase boundary condition at the bottom of the bed is equally straightforward:

$$\text{At } z = L,\ t > 0,\ \frac{\partial p}{\partial z} = 0. \tag{12}$$

At the top of the bed, gas flows into the void above the bed at a constant rate; however, the flux into the bed itself changes with time.

A material balance around the void space above the sorbent bed yields

$$I - FA = \frac{V}{RT_a}\frac{\partial p}{\partial t}. \tag{13}$$

The flux into the bed, based on the total cross-sectional area, is given by

$$F = \epsilon v c. \tag{14}$$

Eliminating v (using Eq. 5) and writing c as a function of pressure using the ideal gas law, Eq. 14 yields

$$F = -\frac{\epsilon\kappa}{RT_b}\frac{\partial p}{\partial z}. \tag{15}$$

Combining Eqs. 13 and 15, the boundary condition at the top of the bed is

$$I + \frac{\epsilon\kappa A}{RT_b}\frac{\partial p}{\partial z} = \frac{V}{RT_a}\frac{\partial p}{\partial t}. \tag{16}$$

Dimensionless variables for time, bed position, pressure, and solid loading may be defined by

$$\theta = \frac{\kappa t}{L^2},$$

$$Z = \frac{z}{L},$$

$$x = \frac{p}{p_R}, \text{ and}$$

$$\bar{y} = \frac{\rho_B RT_b \bar{q}}{p_R \epsilon},$$

respectively, where p_R is a reference pressure. In dimensionless terms, Eqs. 8 through 16 become

$$\frac{\partial x}{\partial \theta} + \frac{\partial \bar{y}}{\partial \theta} - \frac{\partial^2 x}{\partial Z^2} = 0, \tag{17}$$

$$\frac{\partial \bar{y}}{\partial \theta} = \frac{15DL^2}{\kappa S^2}(y_s - \bar{y}), \tag{18}$$

$$y_s = \frac{\rho_B RT_b}{P_R \epsilon}\frac{q_m k p_R x}{1 + k p_R x}, \tag{19}$$

$$\bar{y} = 0 \text{ and } x = 0 \text{ for } \theta = 0 \text{ and } 0 \le Z \le 1, \tag{20}$$

$$\frac{\partial x}{\partial Z} = 0 \text{ for } \theta > 0 \text{ and } Z = 1, \text{ and} \tag{21}$$

$$I + \frac{\epsilon\kappa A p_R}{RT_b L}\frac{\partial x}{\partial Z} = \frac{V p_R \kappa}{RT_a L^2}\frac{\partial x}{\partial \theta} \text{ for } \theta > 0 \text{ and } Z = 0. \tag{22}$$

Equations 17 through 22 were solved by a finite-difference procedure. Finite-difference equations were written in the Crank-Nicholson formulation, and simultaneous equations over the bed cross section were solved for each increment of bed length by matrix inversion. Details of the numerical formulation are given by Crabb (1984).

EXPERIMENTAL

A schematic drawing of the experimental system is shown in Figure 2. Gas flows from a pressurized cylinder through either of two stainless steel calibrated orifices connected in parallel. The leak rate through the orifices is determined by the pressure maintained in the feed line. For nitrogen, leak rates of 2.7×10^{-9} to 3.6×10^{-8} mol/s result as the pressure is increased from 6.89×10^4 to 6.89×10^5 Pa; for carbon dioxide, the corresponding range is 3.0×10^{-9} to 3.9×10^{-8} mol/s.

From the leaks, gas is directed to one of two bed holders. The holder shown on the left was used in preliminary experiments but not in the runs reported here. When directed to the right, gas flows both to the bed section and to tubing to which differential pressure cells are attached. The bed section is a 21 cm piece of 0.77 cm I.D. stainless steel tubing. The ends are covered with fine-mesh screen to prevent the escape of molecular sieves from the bed. Five 0.16 cm O.D. tubes connect the bed to the differential pressure cells to allow measurement of the pressure drop across the bed at various points.

The seven capacitance manometers are connected to electronics and digital readout units that feed to an Apple II+ microcomputer. A computer code was developed to record the absolute pressure in the system above the bed as well as the pressure drops across the bed at regular time increments. A vacuum of about 10^{-3} torr (0.133 Pa) can be maintained in this system.

The sorbent was a type 4A synthetic zeolite molecular sieve obtained from the Davison Chemical Division of W. R. Grace and Co. A batch of 14 to 40 mesh spherical pellets was separated into various sized cuts using wire mesh screens. In two series of runs, pellets with diameters ranging from 0.50 to 0.60 mm (30 to 35 mesh) and from 0.60 to 0.85 mm (20 to 30 mesh) were used.

Although the pellets are described as spherical, in a given sample they may vary significantly from sphericity. Electron microscope photographs showed zeolite crystals of various sizes and shapes are held together by a binder. From such photographs, determinations were made of the crystal size distribution; the mean crystal size was 1.85 μm.

To begin a run, the bed section was heated at 300°C for about 24 h to insure that the sorbent was clean and dry; the system was evacuated during this time using an external pump. After air cooling to room temperature, the bed was submerged in a liquid coolant. Finally, the system was isolated from the external pump.

After about 1 h, when the system pressure steadied (at about 10^{-3} torr), the valve from the gas cylinder to the bed was opened and data collection begun. Data were collected until the bed was saturated with gas, as indicated by a sharp increase in system pressure and a decrease in pressure drop across the bed, or until the system pressure reached 1 torr (133 Pa). The system was then returned to room temperature, using the external pump to evacuate the desorbing gas.

RESULTS

Four series of experimental runs were conducted with nitrogen and carbon dioxide in which the major variables were the

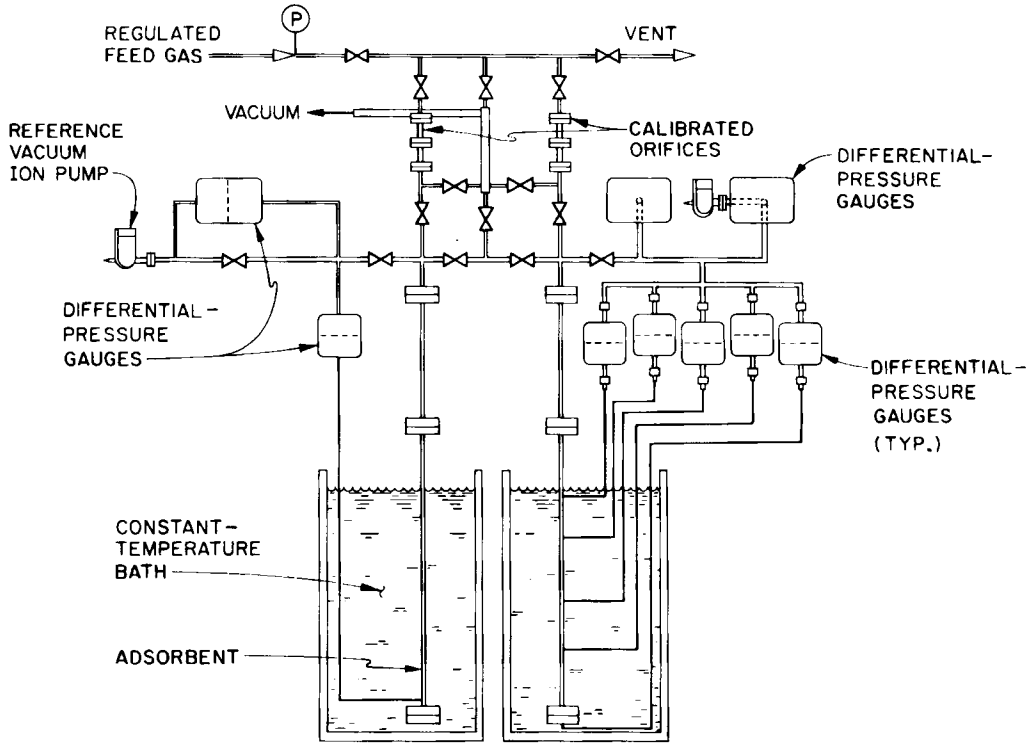

Figure 2. Diagram of experimental sorption pumping apparatus.

flow rate of gas into the system and the sorbent particle size. Figures 3 and 4 present the results of runs with N_2 in which the leak rates were 1.2×10^{-8}, 2.5×10^{-8}, and 3.0×10^{-8} mol/s and the average particle diameter was either 0.55 or 0.72 mm; the bed was cooled with liquid N_2 to 77 K. Figures 5 and 6 show data obtained sorbing CO_2 on similar beds at flow rates of 3.3×10^{-8} and 3.9×10^{-8} mol/s, with a bed temperature of 198 K maintained using dry ice in acetone. Table 1 summarizes the run conditions.

Figures 3 and 4 show the experimental pressure values for the ambient-temperature void above the sorbent bed as a function of time for the six N_2 runs with average pellet sizes of 0.55 mm and 0.72 mm, respectively. The pressure vs. time profiles are similar for all runs, with initial linear increases in the void pressure as gas is pumped into the bed at a constant rate. As the bed nears saturation, flow into the bed decreases and the pressure increases rapidly.

Typical pressure-drop data for experimental runs with nitro-

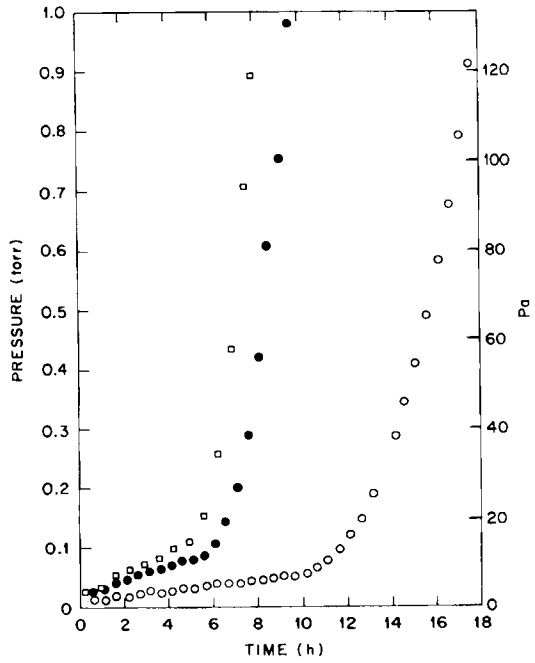

Figure 3. Sorption of N_2 on 0.55 mm 4A sieves. Feed rates, mol/s: ○ 1.2×10^{-8}; ● 2.5×10^{-8}; □ 3.0×10^{-8}.

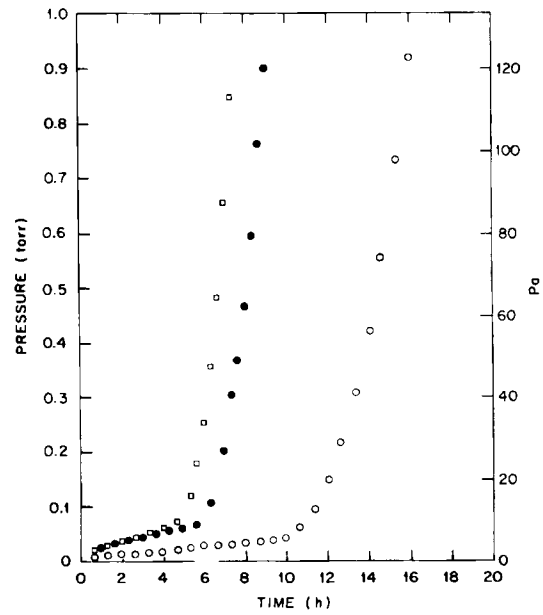

Figure 4. Sorption of N_2 on 0.72 mm 4A sieves. Feed rates, mol/s: ○ 1.2×10^{-8}; ● 2.5×10^{-8}; □ 3.0×10^{-8}.

Table 1. Experimental Conditions for Sorption Pumping of N_2 and CO_2 on Davison 4A Sieves

Sorbent Bed Parameters				Flow Rate of Gas into Void above Bed 10^{-8} mol/s
Particle Dia. mm	Mass g	Height cm	Coolant Temp. K	
		N_2		
0.50–0.60	5.06	11.6	77	1.2
0.50–0.60	5.06	11.6	77	2.5
0.50–0.60	5.06	11.6	77	3.0
0.60–0.80	4.12	9.5	77	1.2
0.60–0.80	4.12	9.5	77	2.5
0.60–0.80	4.12	9.5	77	3.0
		CO_2		
0.50–0.60	4.69	10.8	198	3.3
0.50–0.60	4.69	10.8	198	3.9
0.60–0.80	4.33	10.0	198	3.3
0.60–0.80	4.33	10.0	198	3.9

gen are shown in Figures 7 and 8. For the period of linear pressure increase, very little gas penetrates to the bottom of the bed, and the pressure drop is high. By the time gas reaches the bottom, the bed is near saturation. As flow into the bed slows, the pressure drop decreases rapidly and the pressure equalizes throughout the system before beginning its sharp rise.

Figures 7 and 8 also show the pressure and pressure-drop curves generated using the numerical solution of the theoretical model. The model requires values of the following parameters: ϵ, ρ_B, T_a, T_a, S, L, V, I, κ, D, q_m, and k. Table 2 lists the values used to calculate the curves shown in these figures.

The experimental pressure vs. time profiles from the two series of runs conducted with CO_2 are presented in Figures 5 and 6. There are major quantitative and qualitative differences between the sorption pumping behavior of N_2 and that of CO_2, the outstanding one being the much greater capacity of the sieves to adsorb CO_2. For example, the pressure above the sorbent bed reached 100 Pa in about 7.5 h when sorbing N_2 at a flow rate of 3.0×10^{-8} mol/s, while more than 135 h were

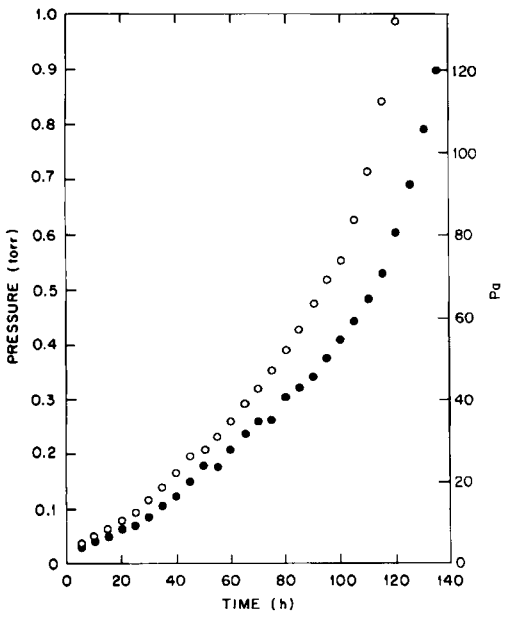

Figure 5. Sorption of CO_2 on 0.55 mm 4A sieves. Feed rates, mol/s: ● 3.0×10^{-8}; ○ 3.6×10^{-8}.

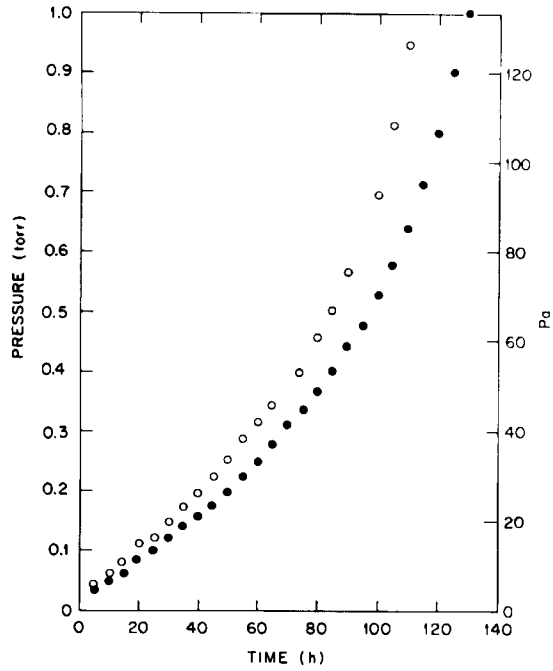

Figure 6. Sorption of CO_2 on 0.72 mm 4A sieves. Feed rates, mol/s: ● 3.0×10^{-8}; ○ 3.6×10^{-8}.

required to reach 100 Pa when sorbing CO_2 at 3.3×10^{-8} mol/s. With CO_2, the pressure rises at a gradually increasing rate, without the period of linear pressure increase characteristic of the N_2 curves.

Figure 9 presents typical pressure-drop data for CO_2. Almost from the outset the absolute value of the pressure drop is less than the total pressure above the bed, indicating that some CO_2 penetrates to the bottom. The pressure drop increases steadily until the bed begins to approach saturation. Theoretical curves using the parameter values in Table 2 are also shown in Figure 9.

COMPARISON WITH THEORETICAL MODEL

Generating pressure and pressure-drop curves using the numerical solution of the theoretical model requires values for

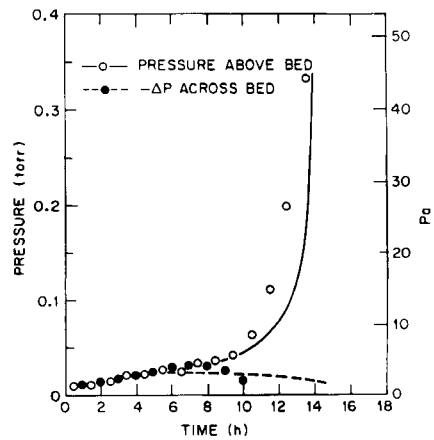

Figure 7. Pressures and pressure drops for N_2 sorption of 0.72 mm 4A sieves at a feed rate of 1.2×10^{-8} mol/s; lines calculated by theoretical model.

Table 2. Parameters Used to Calculate Theoretical Pressure and Pressure-drop Curves for N_2 and CO_2*

T_b K	D m²/s	k Pa⁻¹	q_m mol/kg	κ m³/s	S m	L m	I 10^{-8} mol/s
				N_2			
77	5×10^{-12}	0.60	0.16	8.0×10^{-3}	2.7×10^{-4}	0.1165	1.2
							2.5
							3.0
				1.05×10^{-2}	3.6×10^{-4}	0.0949	1.2
							2.5
							3.0
				CO_2			
198	1.1×10^{-17}	0.0375	4.0	2.00×10^{-2}	(0.92×10^{-6})**	0.108	3.3
							3.9
				2.00×10^{-2}	(0.92×10^{-6})**	0.0997	3.3
							3.9

* For all runs, $\epsilon = 0.35$, $\rho_B = 920$ kg/m³, $T_a = 300$ K, and $V = 2\times10^{-4}$ m³.
** Average crystal size used in model for CO_2, rather than pellet size.

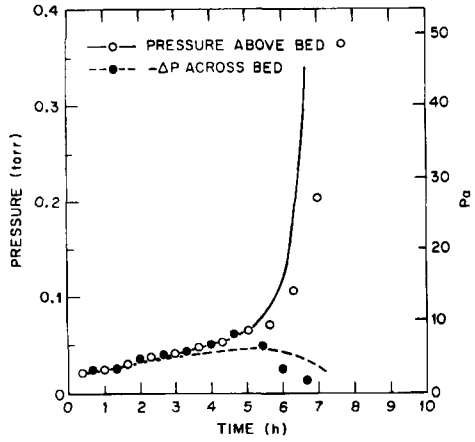

Figure 8. Pressures and pressure drops for N_2 sorption of 0.72 mm 4A sieves at a feed rate of 2.5×10^{-8} mol/s; lines calculated by theoretical model.

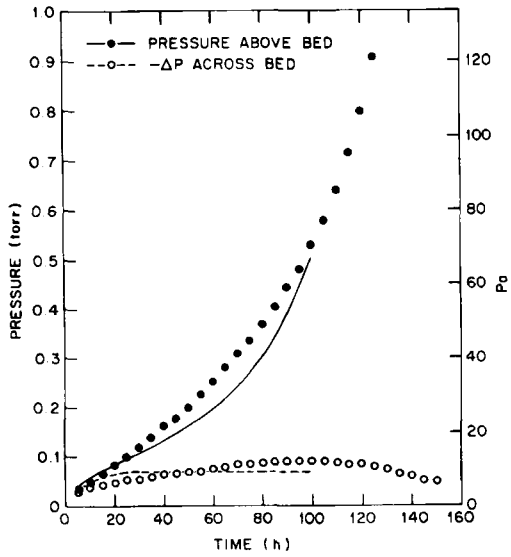

Figure 9. Pressures and pressure drops for CO_2 sorption on 0.72 mm 4A sieves at a feed rate of 3.3×10^{-8} mol/s; lines calculated by theoretical model.

twelve parameters. Eight of these parameters, $\epsilon, \rho_B, T_a, T_b, V, S, L$, and I, are either properties of the sorbent or experimental conditions that can readily be measured or estimated. The bulk density was obtained by weighing a measured volume of the sorbent particles, and the void fraction was estimated for spherical particles. Calculated pressure curves were found to be fairly insensitive to T_a, and a value of 300 K was used.

Choosing the values of D, k, q_m, and κ that best fit the theoretical curves to the experimental data was made easier by the observation that a change in any of the four has a marked effect on either the theoretical pressure curve or pressure-drop curve. For example, D is the only one of the four parameters that affects the magnitude of the initial pressure increase at the start of a run. A change in k alters the slope of the linear portion of the pressure curve; q_m determines when the pressure profile will break upward; and κ most significantly affects the magnitude of the pressure drop across the bed.

The solid-phase diffusivity, D, for gas-zeolite systems is related to temperature through an Arrhenius equation (Ruthven and Derrah, 1975):

$$D = D^* \exp(-E/RT). \tag{23}$$

Several sets of values for the preexponential factor, D^*, and the activation energy, E, are available in the literature for N_2 and CO_2 in 4A sieves. Table 3 lists diffusivities calculated from Eq. 23 for N_2 at 77 K and CO_2 at 198 K. For N_2, the calculated values range from 4.0×10^{-24} to 5.9×10^{-21} cm²/s; for CO_2, the values are 7.5×10^{-12} and 1.2×10^{-13} cm²/s.

Table 3. Extrapolated Values of Diffusivity in Zeolite Type 4A Crystals

Calculated D m²/s	Source of Data	Temp. Range of Experiments K
	Experimental, N_2 at 77 K	
4.0×10^{-28}	Ruthven and Derrah (1975)	215–277
6.1×10^{-25} -4.0×10^{-26}	Roques and Bastick (1970)	90–160
5.9×10^{-25}	Habgood (1958)	194 and 273
	Experimental, CO_2 at 198 K	
7.5×10^{-16}	Yucel and Ruthven (1980) (own 4A)	273–371
1.2×10^{-17}	Yucel and Ruthven (1980) (Linde 4A)	323–385

The solid-phase diffusivity value is used in the model equation only where it is coupled with the sphere radius (i.e., Eq. 18). For CO_2, the best value for D/S^2 (1.3×10^{-5} s^{-1}) represents an effective diffusivity of 1.1×10^{-13} cm^2/s if the mean crystal size of 1.85 μm is used in the model equations. This is in good agreement with the extrapolated values given in Table 3.

In the nitrogen experiments, saturation was approached in less than 15 h in all runs. With crystal diffusivities of the order shown in Table 3, Fourier numbers (Dt/S^2) of less than 10^{-13} are predicted, indicating that an extremely small degree of penetration of the crystals by nitrogen occurs. Thus the observed value for D of 5×10^{-12} m^2/s is based on the overall particle diameter. It provides the best fit of the theoretical curves to the experimental and applies to diffusion within the macropores.

The significant difference between the behavior of N_2 and CO_2 probably results partially from differences in the temperatures used. Experiments with both N_2 and CO_2 were near the condensation temperatures of the respective gases, but the N_2 experimental temperature was thus much lower. Under these conditions, the condensed phase of the N_2 is a liquid, and surface tension could enhance the N_2 condensation in macropores. This would not be true for the CO_2.

Searching the literature for estimates of k and q_m, the constants required in the Langmuir adsorption isotherm equation, reveals no data for the N_2-4A system at low temperatures and pressures in the range of interest. The values of 0.60 Pa^{-1} for k and 0.16 mol/kg for q_m gave the best fit of the model equations to the experimental data.

Equilibrium adsorption data for CO_2 on 4A sieves at 198 K were provided by the manufacturer over the range 266 to 5×10^4 Pa. The data from 266 to 1.33×10^3 Pa were used to estimate k and q_m; the estimated values are 0.0375 Pa^{-1} and 4.0 mol/kg. These values worked well in the model equations.

A first-order estimate of κ can be made through the following approximation:

$$\left(\frac{H}{A^2}\right)_{avg} A_{avg} \cong \left(\frac{H}{A}\right)_{avg} = \frac{4}{D_H}. \tag{24}$$

The hydraulic diameter for a packed bed may be calculated (Bird et al., 1960)

$$D_H = \frac{4S\epsilon}{3(1-\epsilon)}. \tag{25}$$

Utilizing Eq. 24 in the definition of κ,

$$\kappa \cong \frac{1}{3} v_m D_H. \tag{26}$$

From Eq. (26), values of κ for N_2 are estimated at 1.6×10^{-2} and 2.1×10^{-2} m^2/s for the two pellet sizes, compared to the experimentally obtained best fit values of 8.0×10^{-3} and 1.05×10^{-2} m^2/s (Table 2). Agreement between the estimated and experimental values is of the expected order. The value of κ is proportional to pellet radius.

For CO_2, values of κ estimated by Eq. (26) are 2.05×10^{-2} and 2.65×10^{-2} m^2/s. Experimental values by the best fit method cannot be obtained with a great deal of precision for CO_2. A value of 2.00×10^{-2} m^2/s was used to generate the model curves in Figure 9 for 0.72 mm pellets, and the fit to the experimental data is reasonably good. However, the model curve of pressure drop is flatter than the experimental curve, and a value of about 3.5×10^{-2} m^2/s yields a better fit over the first 20 h of the run. This lack of precise fit for the CO_2 pressure-drop data probably stems from the representation of the range of zeolite crystal sizes by a uniform spherical geometry in the model.

In summary, sorption pumping data were obtained for N_2 and CO_2, and the data were represented reasonably well by a simple theoretical model. In addition, estimates were obtained for diffusivities and equilibrium parameters at low temperatures and pressures. A new transport parameter for molecular flow in packed beds, κ, was defined and estimated.

ACKNOWLEDGMENT

This research was sponsored by the Office of Basic Energy Sciences, U.S. Department of Energy under contract DE-AC05-840R21400 with Martin Marietta Energy Systems, Inc.

NOTATION

A = channel or bed cross-sectional area, cm^2
c = fluid-phase concentration, mol/cm^3
D = effective solid-phase diffusivity, cm^2/s
D^* = preexponential factor for diffusion, cm^2/s
D_H = hydraulic diameter of channel, cm
E = energy of activation for diffusion, kcal/mol
F = mass flux into bed, $mol/cm^2 \cdot s$
H = channel perimeter, cm
I = constant mass flow rate into void above bed, mol/s
k = Langmuir isotherm constant, $torr^{-1}$ (13.3 Pa)
L = channel or bed length, cm
P = fluid-phase pressure, torr (133 Pa)
q = solid-phase concentration at r
$\bar{q}$ = average solid-phase concentration, mol/g
q_m = Langmuir isotherm constant, mol/g
q_S = solid-phase concentration at sorbent particle surface, mol/g
Q = gas throughput, $torr \cdot cm^3/s$ (133 $Pa \cdot cm^3/s$)
r = radial position in particle, cm
R = universal gas constant, $torr \cdot cm^3/mol \cdot K$ (133 $Pa \cdot cm^3/mol \cdot K$)
S = sorbent particle radius, cm
t = time, s
T = absolute temperature, K
T_a = absolute ambient temperature, K
T_b = absolute temperature of sorbent bed, K
v = fluid velocity, cm/s
v_m = average molecular velocity, cm/s
V = volume, cm^3
V_f = volumetric flow rate, cm^3/s
x = dimensionless variable for pressure
$\bar{y}$ = dimensionless variable for average solid-phase concentration
z = axial position in bed, cm
Z = dimensionless variable for axial position in bed

Greek Letters

ϵ = void fraction of bed, cm^3 void/cm^3 bed
θ = dimensionless variable for time
κ = interstitial mass transfer coefficient, cm^2/s
ρ_B = bulk density of sorbent, g/cm^3

LITERATURE CITED

Bird, R. B., W. E. Stewart, and E. N. Lightfoot, *Transport Phenomena*, Wiley, New York, 197 (1960).

Crabb, K. S., "Mass Transfer in Vacuum Sorption Pumping of Pure Gases on Molecular Sieves," M.S. Thesis, Univ. of Tennessee, Knoxville (1984).

Fisher, P. W., and J. S. Watson, "Cryosorption Pumping of Deuterium

by MS – 5A at Temperatures above 4.2 K for Fusion Reactor Applications," *J. Vac. Sci. Technol.*, 15(2), 741 (1978).
Garg, D. R., and D. M. Ruthven, "Theoretical Prediction of Breakthrough Curves for Molecular Sieve Adsorption Columns. I: Asymptotic Solutions," *Chem. Eng. Sci.*, **28**, 791 (1973).
Garg, D. R., and D. M. Ruthven, "Linear Driving Force Approximations for Diffusion-Controlled Adsorption in Molecular Sieve Columns," *AIChE J.*, **21**, 200 (1975).
Glueckauf, E., "Theory of Chromatography. 10: Formulae for Diffusion into Spheres and Their Application to Chromatography," *Trans. Faraday. Soc.*, **51**, 1,540 (1955).
Habgood, H. W., "The Kinetics of Molecular Sieve Action. Sorption of Nitrogen-Methane Mixtures by Linde Molecular Sieve 4A," *Can. J. Chem.*, **36**, 1,384 (1958).
Knudsen, M., "Molecular Flow of Gases through Apertures and Effusion," *Ann. Physik.*, **28**, 999 (1909).
Liaw, C. H., et al., "Kinetics of Fixed-Bed Adsorption: A New Solution," *AIChE J.*, **25**, 376 (1979).
Perona, J. J., et al., "Vacuum Sorption Pumping Studies of Nitrogen on Molecular Sieves," AIChE Ann. Meet. Washington, D.C., Paper No. 52d (1983).
Roques, M., and M. Bastick, *Bull. Soc. Chim.*, France, 1,272 (1970).
Ruthven, D. M., and R. I. Derrah, "Diffusion of Monatomic and Diatomic Gases in 4A and 5A Zeolites," *J. Chem. Soc. Faraday Trans.* **I**, **71**, 2,031 (1975).
Ruthven, D. M., and K. F. Loughlin, "Correlation and Interpretation of Zeolite Diffusion Coefficients," *Trans. Faraday Soc.*, **67**, 1,661 (1971a).
——, "The Effect of Crystallite Shape and Size Distribution on Diffusion Measurements in Molecular Sieves," *Chem. Eng. Sci.*, **26**, 577 (1971b).
Tung, C. P., "Sorption Pumping of Gases by Deep Beds of Sorbents," Ph.D. Dissertation, Univ. of Tennessee, Knoxville (1977).
Yucel, H., and D. M. Ruthven, "Diffusion of CO_2 in 4A and 5A Zeolite Crystals," *J. Coll. Int. Sci.*, **74**, 186 (1980).

Manuscript received Nov. 29, 1984, and revision received Apr. 23, 1985.